RHEOLOGICAL AND MICROSTRUCTURAL STUDY OF A356 ALLOY SOLIDIFIED UNDER MAGNETIC STIRRING

O. Bustos and S. Ordoñez
University of Santiago de Chile, Department of Metallurgical Engineering, Santiago, Chile

R. Colás
Autonomous University of Nuevo León, Faculty of Mechanical and Electrical Engineering, San Nicolas de los Garza, Nuevo Leon, Mexico

Abstract

Results on the rheological behavior of an A356 alloy compressed between parallel plates in the semisolid state are presented in this work. The tests were performed on cylindrical specimens machined from billets cast while being subjected to a rotating permanent magnetic field. These samples did not exhibit the conventional microstructure of dendrites, and were tested with different solid fractions. The tests were performed either at a constant load or at a constant displacement rate. A power law equation was derived to describe the rheological behavior of the material when tested at constant load, however, it was not possible to establish a mathematical relationship to describe the flow on the semisolid material when the tests were made at constant displacement rate. It can be concluded from these results that the rheological behavior of the alloy is affected by the morphology of the phases present in the microstructure, in such a way that a globular microstructure, with a shape factor near the unit, behaves as a fluid while deformed in the semisolid state, a behavior that is not witnessed in an as-cast dendritic microstructure.

Keywords: *solidification, magnetic stirring, microstructure, rheology*

Introduction

The use of magnetic fields during metal solidification dates from the 1930s decade. Magnetic stirring, in the electromagnetic cast, is due to the Lorentz forces generated by an alternating inductor. Magnetic stirrers are designed to produce convection in the liquid near the solidification front, and this is the reason for the use of low frequency magnetic fields that allow for Lorentz forces to penetrate deeply into the liquid metal.1

In a Newtonian fluid, the shear stress, τ, is proportional to the shear rate, $\dot{\gamma}$, and the constant of proportionality is the viscosity, η. Thixotropic fluids are non-Newtonian, i.e., the shear stress is not proportional to the shear rate. The viscosity is then named "apparent viscosity" and depends on shear rate, pressure, temperature and time. Some non-linear fluids also show viscoelasticity i.e., they store some of the mechanical energy as elastic energy. Thixotropic materials do not store elastic energy and show no elastic recovery when the stress is removed. If a fluid exhibits a yield stress and then gives a linear relationship between shear stress and shear rate, it is termed a Bingham material.2 Then,

$$\tau = \tau_y + k\dot{\gamma} \qquad \text{Eqn. 1}$$

where k is a parameter related to viscosity. The Herschel–Bulkley model is applied when behavior is non-linear after yield i.e.:

$$\tau = \tau_y + k\dot{\gamma}^n \qquad \text{Eqn. 2}$$

The Ostwald-de-Waele relationship is used to describe fluids which do not have a yield point and where a power law relationship between the shear stress τ and the shear rate γ can be established.[2]

$$\tau = k\dot{\gamma}^n \qquad \text{Eqn. 3}$$

If the exponent n is equal to 1, this expression is reduced to a Newtonian fluid with the parameter k equal to viscosity. A shear thinning material (in which viscosity decreases as the shear rate increases) would have a value of n of less than 1, and a shear thickening material would have n greater than 1.

Joly and Mehrabian used a simple power law to describe the shear thinning behavior observed during isothermal steady state experiments:[2]

$$\eta = k\dot{\gamma}^{m-1} \qquad \text{Eqn. 4}$$

Where: η is the apparent viscosity, $\dot{\gamma}$ is the shear rate, and k and m are two solid fraction dependent factors.

The non-Newtonian, two parameter, Ostwald-de-Waele or power law model is widely used to describe the rheological behavior of pseudoplastic materials. This model assumes a relationship of the form,

$$\mu = m\dot{\gamma}^{(n-1)} \qquad \text{Eqn. 5}$$

Where: m and n are experimentally determined coefficients.

Laxmanan and Flemings[3] derived an equation for the case of a sample of constant volume being compressed between two large plates, their final result is:

$$\frac{h_0}{h} = \left\{1 + \left(\frac{3n+5}{2n}\right) h_o^{(n+1)/n}\ kt\right\}^{2n/(3n+5)} \qquad \text{Eqn. 6}$$

Where: h_0 is the initial height, h the instantaneous height, m and n are power law constants and k

$$k = \left\{\left(\frac{2n}{2n+1}\right)^n \frac{4F}{\pi d_o^{n+3}\ m}(n+3)\right\}^{1/n} \qquad \text{Eqn. 7}$$

Where: d_o is initial diameter and F the applied load

It is possible to calculate the power-law parameters m and n using equations (6) and (7). This involves replotting the experimental data using the equation of the engneering strain valid for long times:

$$e = \left(1 - \frac{h}{h_0}\right) = 1 - \left\{1 + \left(\frac{3n+5}{2n}\right) h_o^{(n+1)/n} kt\right\}^{-\left[\frac{2n}{3n+5}\right]} \qquad \text{Eqn.}$$

m and n may be obtained from the slope and intercept of a plot of log (1-e) vs log t at long times.

The aim of this work is to present the results of the study on the rheological behavior of a semisolid aluminum alloy deformed in compression at high temperature in a specially designed machine. The semisolid alloy was subjected to a rotating magnetic field during solidification.

Experimental Procedure

A commercial A356 alloy was used for the experiments, the chemical composition, obtained by optical emission spectroscopy according to ASTM E607-90 specification, was 0.1 Fe, 7 Si and 0.25 Mg, weight %, bal. Al.

The non-dendritic structure was produced using the equipment designed by the authors, which consists in two layers of three permanent magnets displaced 120° from each other. The distance between the layers is 30 mm. The magnets rotate around the crucible with molten metal.[4] Samples of the alloy of around 250 g were melted in ceramic crucibles to a temperature of 680C (1256F) and poured in moulds kept either at 25C (77F) or 200C (392F). Some samples of the alloy were left to solidify freely and others under the influence of a permanent rotary magnetic field. The rotation speeds of the magnetic field were of 0, 650, 980 and 1540 rpm. The cooling curves were recorded to evaluate the effect that stirring exerts on solidification.

Samples from the solid material were prepared following standard metallographic practice to evaluate their grain size, secondary dendritic arm spacing and the size and shape factor of the silicon platelets from the Al-Si eutectic. The samples were etched by a modified Poulton's reagent with the following composition: 50 ml Poulton's reagent (12 ml HCl + 6ml HNO_3 + 1ml HF + 1ml water), 25 ml nitric acid, 12 g chromic acid, and 40 ml water and Keller reagent with the following composition: 5 ml HNO_3 (conc) + 3 ml HCl (conc) + 2 ml HF (48%) + 190 ml water.

Compression tests were carried out on specimens of 12.5 mm in diameter and 7.0 mm in length machined from the solidified samples. These specimens were compressed between parallel plates at either constant displacement rate or constant load. The parameters used in the constant displacement tests are shown in Table 1, whereas the parameters used in the constant load tests are shown in Table 2.

Table 1. Conditions of Compression Test at Constant Displacement Rate

Condition	Displacement rate (mm/s)	Testing temperature C (F)
Without stirring, as cast, mould heated to 200 C (392 F)	0.4	570, 580, 590 (1058, 1076, 1094)
Magnetically stirred at 650 rpm, mould heated to 200 C (392 F)	0.4	570, 580, 590 (1058, 1076, 1094)
Magnetically stirred at 980 rpm, mould heated to 200 C (392 F)	0.4	570, 580, 590 (1058, 1076, 1094)

Results and Discussion

Microstructure

Figure 1 shows the macrostructures of the A356 alloy cast in ceramic moulds either kept at 25C (77F) or heated to 200C (392F), without stirring or stirred by a magnetic field rotating at 1540 rpm. The changes in grain size and distribution produced by magnetic stirring can be appreciated, the as cast grain size of 338 µm was reduced to 136 µm for magnetic stirring at 1540 rpm.

The microstructures shown in Figure 2 correspond to the alloy cast in preheated moulds at 200C (392F) where it can be appreciated that stirring reduces the average grain size (as each grain originates from an individual dendrite) and the secondary dendritic arm spacing; the most important factor may be that the morphology of the dendrites change into that of equiaxed rosettes.

The changes from dendrites to rosettes is due to solidification conditions and the thermal gradients developed within the samples, as has been described by Doherty et. al.[5] and it only depends on the Ostwald ripening rather than on the stirring. Figure 3 shows that magnetic stirring reduces not only the grain size and secondary dendritic arm spacing, it also reduces the size of the silicon platelets.

Table 2. Conditions of Compression Test at Constant Load

Condition	Load (N)	Temperature, C (F)
Without stirring, as cast, mould heated to 200C (392F)	13, 20, 30	570, 580, 590 (1058, 1076, 1094)
Magnetically stirred at 650 rpm, mould heated to 200 C (392F)	13, 20, 30	570, 580, 590 (1058,1076, 1094)
Magnetically stirred at 980 rpm, mould heated to 200 C (392F)	13, 20, 30	570, 580, 590 (1058, 1076, 1094)

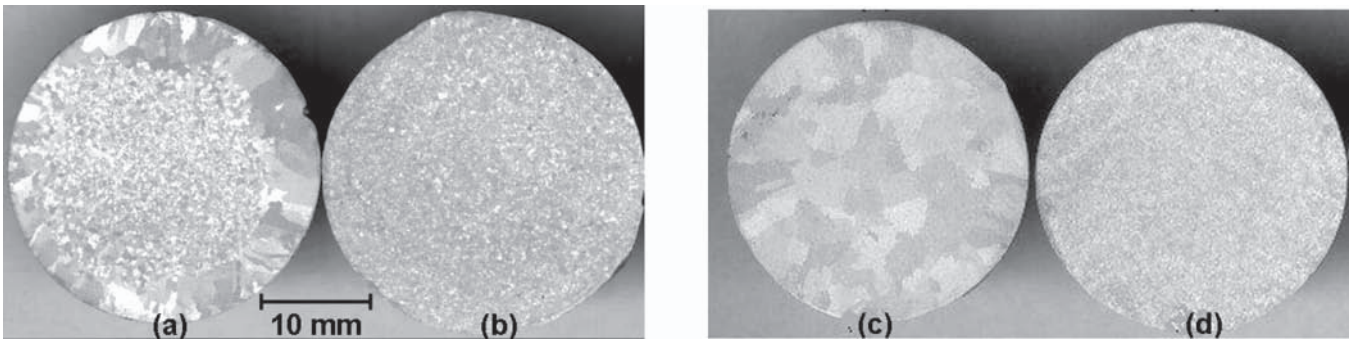

Figure 1. Samples of the A356 alloy cast at in moulds at either 25C (77F) or 200C (392F), without and with the use of the magnetic field rotating at 1540 rpm. (a) no stirring, 25C (77F); (b) stirred, 25C (77F); (c) no stirring, 200C (392F); (d) stirred, 200C (392F).

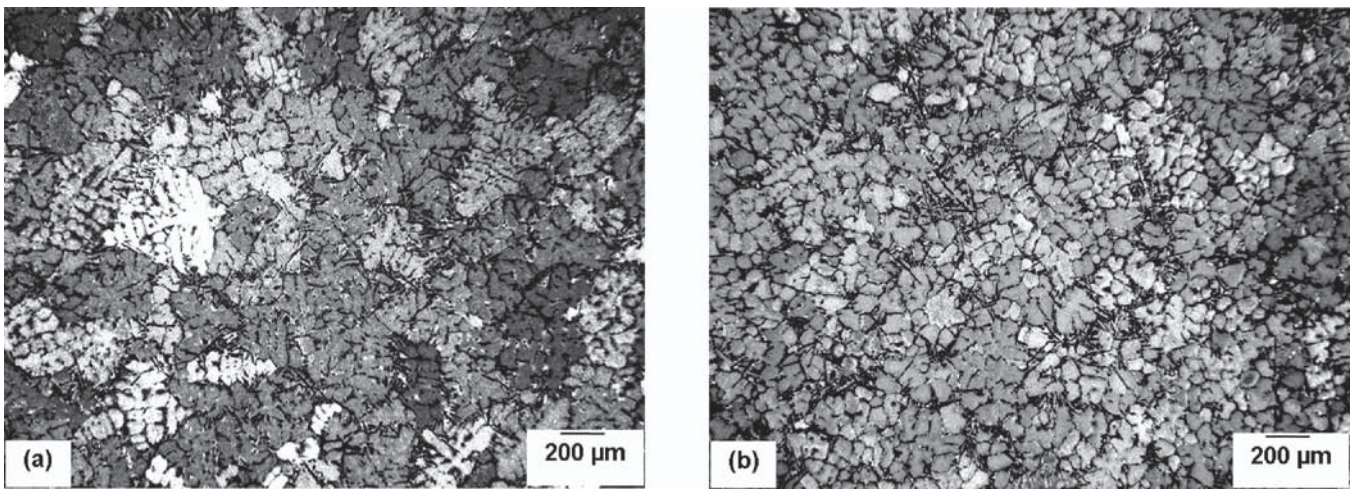

Figure 2. Microstructure of the A356 alloy solidified in a mould heated at 200C (392F) without magnetic stirring (a) or stirred at 1540 rpm (b).

Microstructural refining can be related to solute transport and the development of shear stresses within the slurry that increases with the rise in rotating speed of the magnetic field, product of Lorentz's forces. The reduction in size of the rosette can be appreciated in microstructure (b) of Figure 2, which may be due to an increase in solute gradient in the solid-liquid interface during solidification. These shear stresses produce an increase on constitutional supercooling and consequently the cellular-dendritic growth is favored.[5]

It is generally accepted that grain refinement in agitated semisolid slurries is caused by dendrite fragmentation. Disagreement arises over the question of how dendrite branches detach. There are three major hypotheses:6 (1) dendrite arms detach at the roots; (2) dendrite arms melt off at their roots and (3) repeated plastic bending creates numerous dislocations at the roots of dendrite arms.

Flemings[7] has proposed the mechanisms for the first two hypotheses and a completely different mechanism has been proposed by Vogel et al.[8] and discussed later by Doherty et al.[5] It may be possible for all these mechanisms to occur simultaneously as the solidification, stirring and cooling conditions change. Thickening or ripening processes operate reducing the surface area and high curvature regions are eliminated or reduced by diffusion of solute into the liquid. This process can be accelerated by stirring, since solute transport is improved. With time, stirring promotes the morphological change from dendrites to rosettes containing liquid trapped between the cellular arms and eventually, between spherical particles. When a slurry that already has growing dendrites is cooled at a fast enough rate, ripening process can lead to islands of liquid trapped and unable to escape between solid spheroids. Under these conditions, continuous stirring cannot exert any effect and the reduction in viscosity is limited.

Vogel and Cantor developed a boundary layer model to analyze the effect of stirring on the growth of spherical particles from the liquid.[9] They found that the growing solid-liquid interface becomes more unstable and the dendrites grow at a higher velocity and with a smaller tip when stirred.[10] This apparent disagreement suggests that the non-dendrite microstructure observed during rheocasting can be produced because the diffusion fields of a great number of growing particles overlap.

Vogel et al [8] have proposed a mechanism of dendritic arms fragmentation that promotes grain multiplication and explain the grain refinement produced by liquid stirring. They suggested that dendrite arms bend plastically under the shear stresses created by stirring and this flexion generate dislocations that promote the misorientation within big dendrite arms.

It is possible to point out that formation of globular structures depends on thickening and Ostwald ripening processes, rather than on stirring, a reason that in the present work in which stirring was conducted in continuous cooling conditions, primary aluminum was in the shape of rosettes.

The cooling curves of Figure 4 show that the application of the magnetic field that stirs the melt shift the eutectic trans-

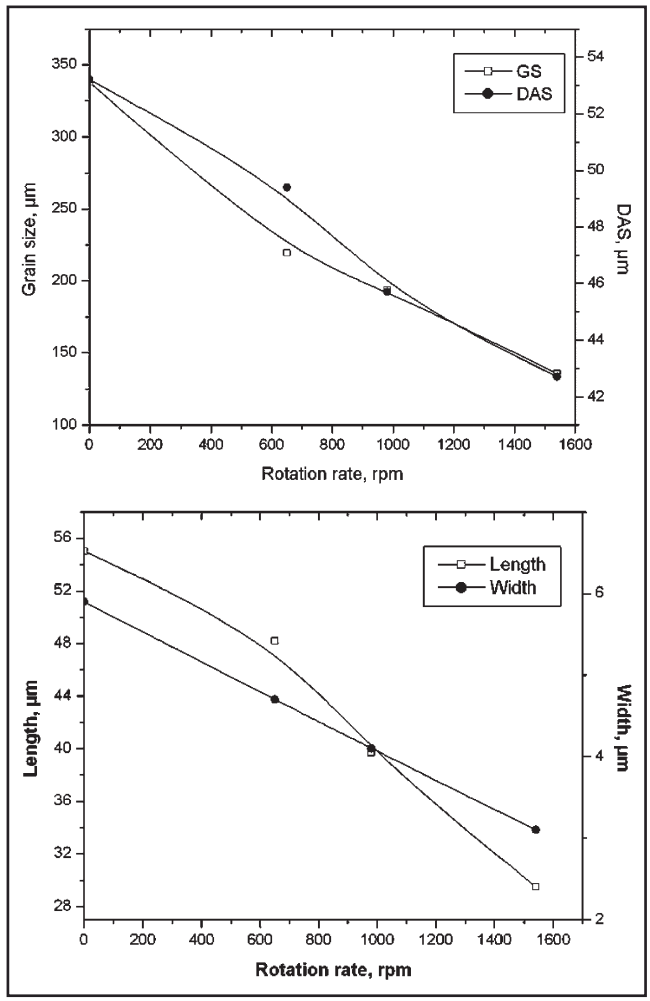

Figure 3. Grain size, DAS, length and width of silicon phase, preheated mould at 200C (392F).

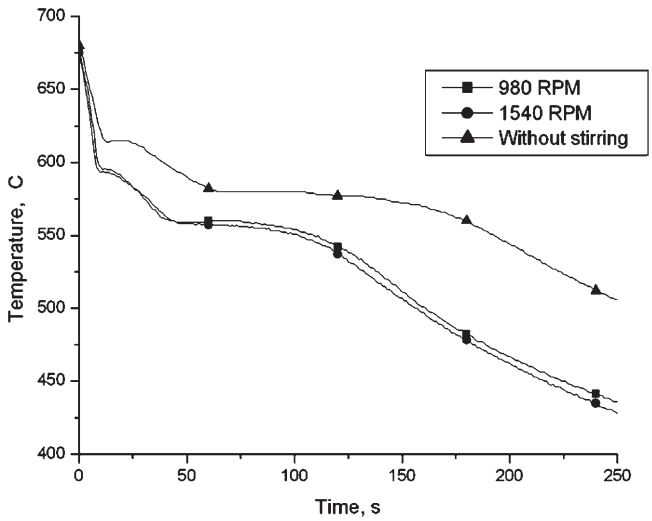

Figure 4. Cooling curves for the A356 alloy for different stirring conditions. The alloy was poured at 680C (1256F) into a crucible held at 200C (392F).

formation point to significantly lower temperatures, which is translated into microstructural refinement. The decrease in temperature for the critical points has been documented by other authors[11-13] and may be attributed to either enhanced convection of the stirred liquid, or to enhanced nucleation from broken dendrites.[14]

Rheology

Four main mechanisms have been proposed to control the deformation of semisolid alloys.[15] Two of them are dominant when the solid particles are surrounded by the liquid phase, and these are the mechanism of liquid flow (LF) and the mechanism of liquid flow that incorporates solid particles (SLF). The other two mechanisms are dominant when the solid particles are in contact with others, and these are the mechanism of sliding between solid particles (SS) and the mechanism of plastic deformation of solid particles (PDS).

Figure 5 shows the behavior of the material while being compressed in the semisolid state at a constant displacement rate of 0.4 mm/s for different processing conditions. The strong incidence of the initial microstructure in the deformation capacity of the materials can be observed. A coarse microstructure (as cast condition), with high connectivity between solid particles, and great amount of liquid trapped between dendrite arms, have a smaller amount of liquid for allowing sliding of particles. This condition strengthens to a greater degree due to liquid expulsion and forcing plastic deformation at the necks of solid. This is the reason for the greater load required for a given degree of deformation, as it is observed in Figure 5.

The samples with non-dendrite microstructures, as is the case for the specimen stirred at 980 rpm, present a pseudoplastic behavior, similar to that of Bingham type fluids, as they only require a small load (between 10 and 20 N) to deform. These materials achieve great deformation without increasing the load until all the liquid is rejected to the periphery of the sample, at such moment, the mechanism changes to plastic deformation at interparticle necks and the load starts to rise,[11] as can be seen in Figure 5.

Figures 6 and 7 show the strain-time curves that describe the rheological behavior of the materials being compressed at constant load (Figure 6) and constant temperature (Figure 7).

Figure 8 shows some of the microstructures found in samples compressed at constant load. It is observed that the only sample that retains a considerable amount of liquid trapped in the interdendritic zones (around 6,8 %vol at 570C [1058F]) is the as cast one, Figure 8(a), but this liquid does not contribute to deformation. Nevertheless, when liquid the liquid fraction increases, the aluminum phase adopts a globular morphology, as result of interparticle sliding and deformation and fragmentation of secondary dendritic arms.[6]

On the other hand, the samples processed via magnetic stirring can be deformed to a great extend, and this is due to the initial expulsion of interparticle liquid to the periphery, Figures 8(c) and 8(e), sliding between solid particles, and plastic deformation of the solid in the center of samples, Figures 8(d) and 8(f).

The experimental data were adjusted to curves that described the rheological behavior of the material according an Ostwald-de-Waele two parameters power law model, it was not possible to establish a relationship to describe the rheological behavior at 570C (1058F) and 580C (1076F), in the

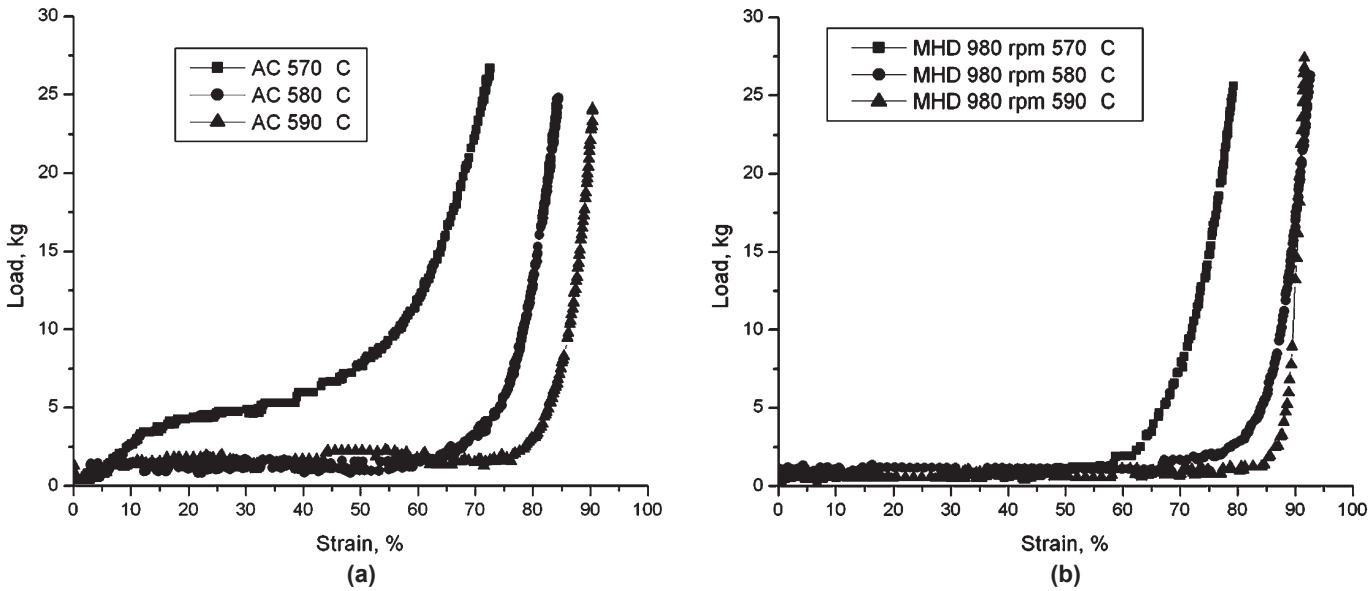

Figure 5. Compression at constant displacement rate between parallel plates for samples in semisolid state; as cast samples (a), samples stirred at 980 rpm (b).

as cast material, due to the the microstructure and amount of liquid available for deformation (Figure 8a), which occurs in a discontinuous way before cracks develop at the surface of the periphery,[10] Figure 9. However, it was possible to describe the rheological behavior by a power law in all the samples that were stirred, even at temperatures as low as 570C (1058F), where a 90% solid fraction, according to the Scheil solidification model, is expected. No cracking was observed in these samples.

The rheological behavior of the material under several processing conditions was determined, using equations (4) and (5) and the model developed by Laxmanan and Flemings.[3] The results are shown in Table 3 and Figure 10. It can be seen that the as cast material and the sample stirred at 1540 rpm present a rheological behavior that evolves from thinning shear to thickening shear when the load applied and the testing temperature increase. The behavior of thickening shear (increase of viscosity with the increase of the shear stress) can be explained by considering that the shear stress field generated in a semi-solid slurry develops a speed gradient through particles of the primary phase. Nevertheless, the particles can move through the fluid at a unique rate. Therefore, the rate gradient generated in the fluid causes rotation of the solid phase. The energy used for this rotation diminishes the energy available for liquid flow, which translates in the increase in the viscosity.

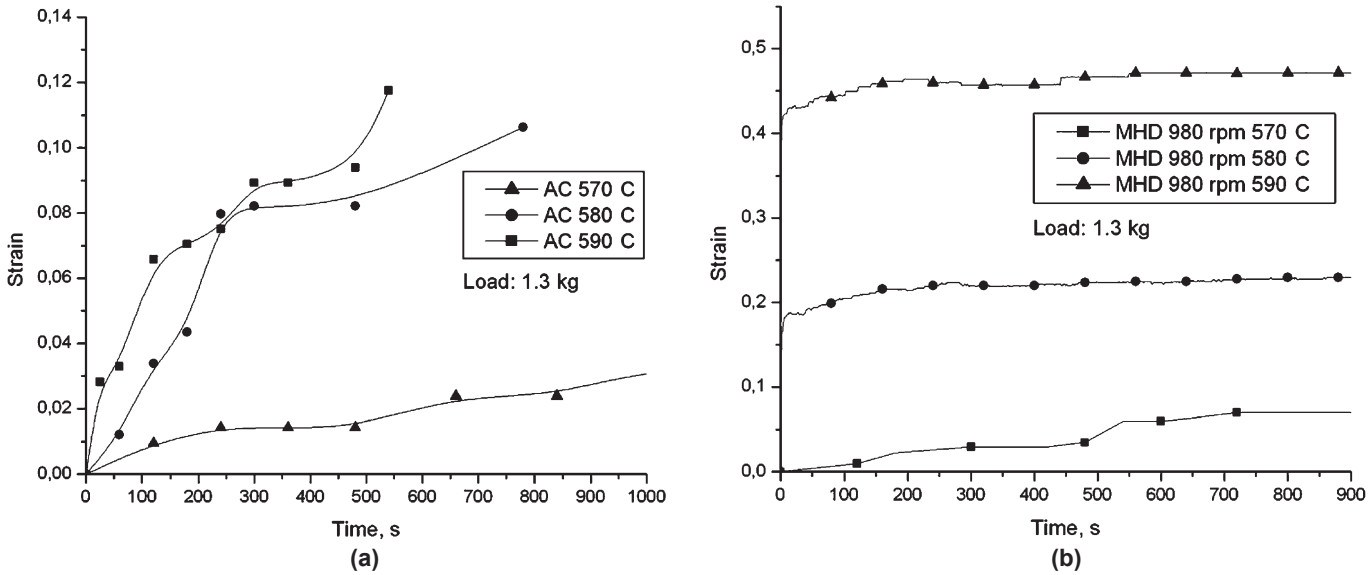

Figure 6. Effect of temperature on the rheological behavior of samples compressed with a constant load of 1.3 kg, (a) as cast, (b) stirred at 980 rpm.

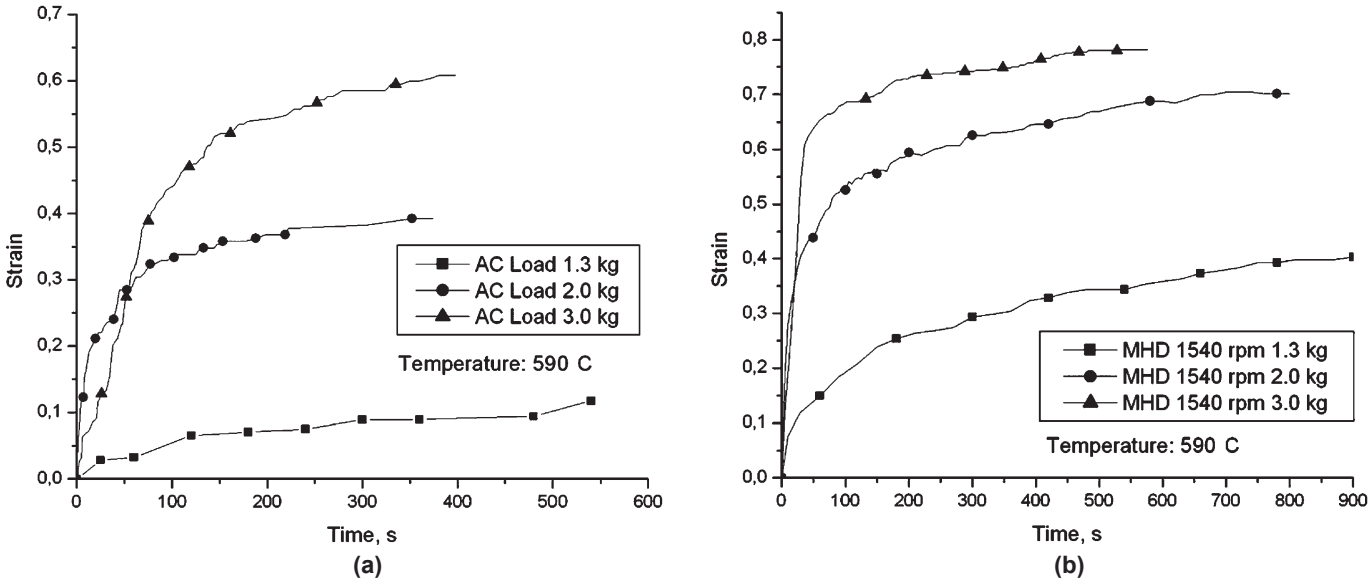

Figure 7. Effect of the applied load on the rheological behavior of samples compressed at 590C (1094F), (a) as cast, (b) magnetically stirred at 1540 rpm.

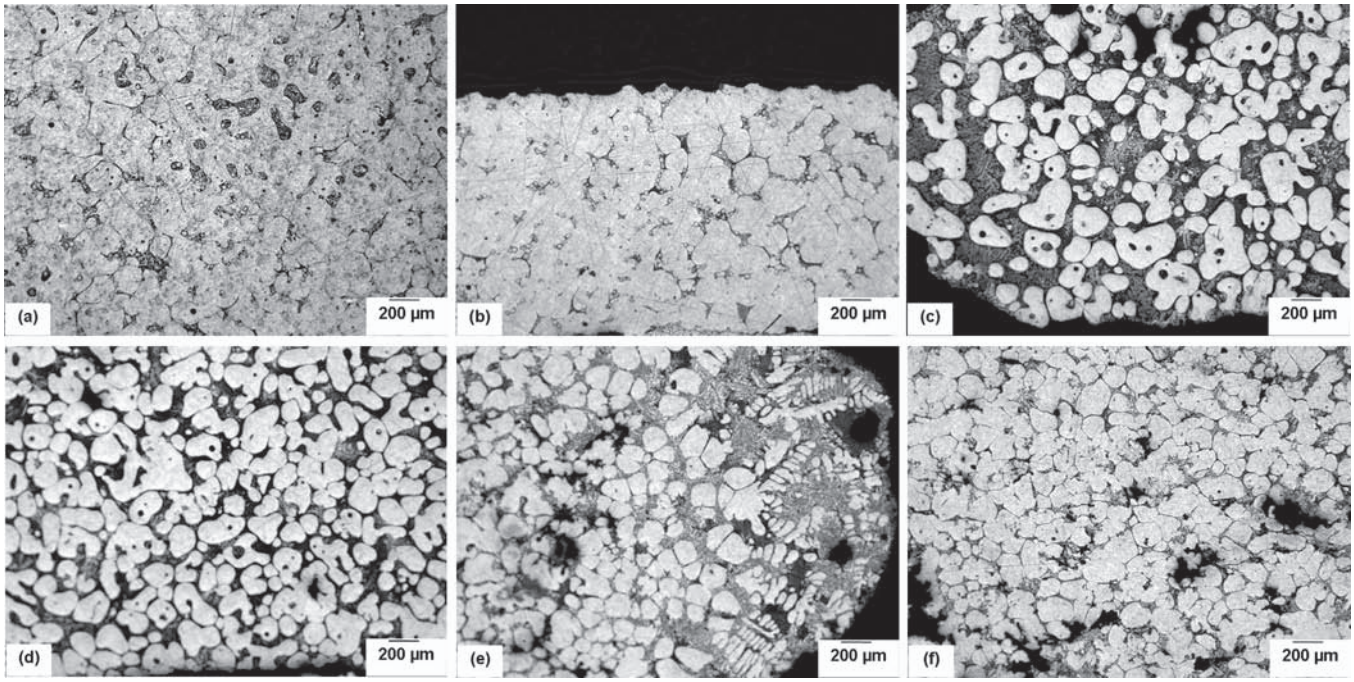

Figure 8. A356 alloy microstructures etched with concentrated Keller reagent compressed with a load of 1.3 kg. (a) as cast sample, deformed at 570C (1058F), central zone; (b) as cast sample, deformed at 590C (1094F), central zone; (c) stirred at 980 rpm sample, deformed at 580C (1076F), edge zone; (d) stirred at 980 rpm sample, deformed at 580C (1076F), central zone; (e) stirred at 1540 rpm sample, deformed at 590C (1094F), edge zone; (f) stirred at 1540 rpm sample, deformed at 590C (1094F), central zone.

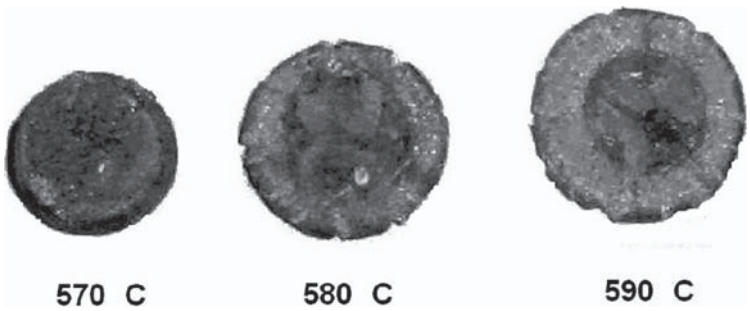

Figure 9. Cracks formation in the as cast material.

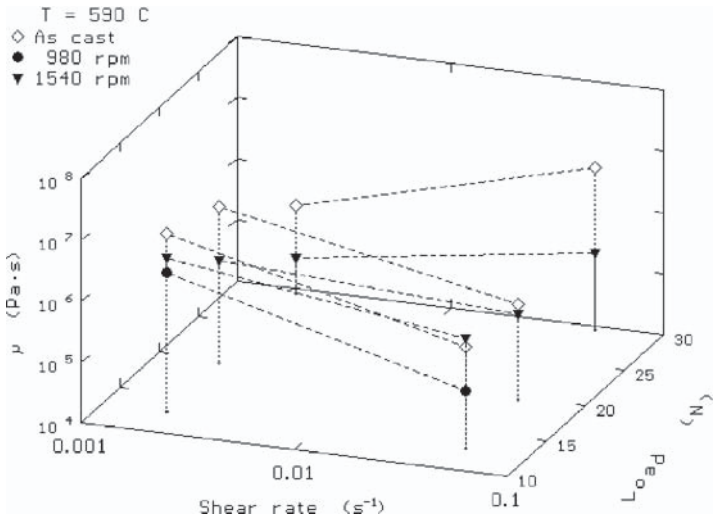

Figure 10. Viscosity-shear rate relationship.

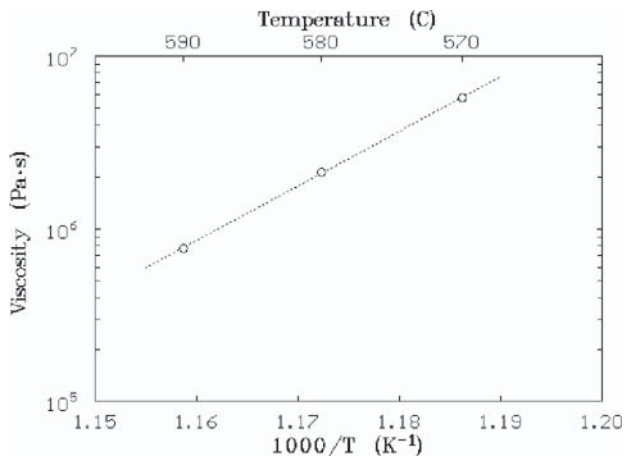

Figure 11. Relationship between viscosity and absolute temperature.

Table 3. Parameters Determine Behavior According to Power Law

Condition	Load (kg)	Temp C (F)	n	m (Pa s)	Log(μ)
As cast	1.3	590 (1094)	0.104	31818.3	6.56
As cast	2.0	590 (1094)	0.287	42632.6	6.27
As cast	3.0	590 (1094)	1.874	62627275	5.79
MHD980	1.3	570 (1058)	0.238	102362.6	6.76
MHD980	1.3	580 (1076)	0.064	14913.6	6.33
MHD980	1.3	590 (1094)	0.051	5101.9	5.89
MHD1540	1.3	590 (1094)	0.479	131499.2	6.32
MHD1540	2.0	590 (1094)	0.806	141253.1	5.60
MHD1540	3.0	590 (1094)	1.477	741636	4.77

The samples cast while stirring at 1540 rpm display a shear thinning type, pseudoplastic behavior. An Arrhenius type relationship exists between the viscosity and the inverse of the absolute temperature, Figure 11, according to:

$$\mu = A \cdot \exp\left(\frac{B}{T}\right) \qquad \text{Eqn. } 9$$

Where $A = 1.12 \cdot 10^{-31}$ (Pa s)
$B = 73211$ (K)

Conclusions

The application of a rotational magnetic field stirs the melt, displace the dendrite and eutectic transformations towards lower temperatures, promoting microstructural refining.

Materials with non-dendritic microstructure, like those that are obtained by stirring via application of magnetic fields, display a pseudoplastic behavior similar to a Bingham type fluid. The material can be deformed to a high extend without significant increases in load until the liquid is expulsed to the periphery. At this point the mechanism responsible for deformation changes to that of straining interparticle necks, consequently the load required to sustain deformation increases.

Samples obtained by magnetic stirring at 1540 rpm exhibit a shear thinning type or pseudoplastic behavior. An Arrhenius type relationship between the viscosity and the inverse of the absolute temperature was established.

Acknowledgements

The authors would like to thank the Chilean National Foundation for Scientific and Technological Development (*Fondo Nacional de Desarrollo Científico y Tecnológico*, FONDECYT), Project 1080133, for the financial support provided.

REFERENCES

1. Antona, L. & Moschini, A., "New Foundry Process for the Production of Light Metals in the Semi-Liquid, Doughy State," *Metallurgical Science & Technology*, vol. 4, pp. 49-59 (1986).
2. Atkinson, H., "Modelling the Semisolid Processing of Metallic Alloys," *Progress in Materials Science*, vol. 50, issue 3, pp. 341-412 (2005).
3. Laxmanan, V., & Flemings, M.C., "Deformation of Semi-solid Sn-15% Pb Alloy", *Metallurgical and Materials Trans. A,* vol. 11, issue 12, pp. 1927-1937 (1980).
4. Leiva, R., Sánchez, C., Mannheim, R., & Bustos, O., "Estudio de la evolución microestructural y comportamiento reológico mediante compresión semisólida entre placas paralelas de la aleación A356 solidificada bajo un campo magnético permanente en rotación", Proc. CONAMET-SAM 2004, La Serena, Chile, pp.651-656.
5. Doherty, R. D., Lee, H. I., & Feest, E. A., "Microstructure of Stir-Cast Metals," *Materials Science and Engineering,* vol. 65, issue 1, pp. 181-189 (1984).
6. Yang, Z., Kang, C. G., & Hu, Z. Q., "Microstructural Stress Concentration: An Important Role in Grain Refinement of Rheocasting Structure," *Metallurgical and Materials Trans. A*, vol. 36, no. 10, pp. 2785-2792 (2005).

7. Flemings, M., "Behavior of Metal Alloys in the Semisolid State," *Metallurgical and Materials Trans. A,* vol. 22, no. 5, pp. 957-981 (1991).
8. Vogel, A., Doherty, R.D., & Cantor, B., "Solidification and Casting of Metals, Proceedings of an International Conference on Solidification, Sheffield 1977 Metals Society, London, pp. 518–524 (1979).
9. Vogel, A. & Cantor, B., "Stability of a Spherical Particle Growing from a Stirred Melt," *Journal of Crystal Growth,* vol. 37, issue 3, pp. 309-316 (1977).
10. Cantor, B. & Vogel, A., "Dendritic Solidification and Fluid Flow," *Journal of Crystal Growth*, vol. 41, issue 1, pp. 109-123 (1977).
11. Griffiths, W.D., & McCartney, C.G, "The Effect of Electromagnetic Stirring During Solidification on the Structure of Al-Si Alloys", *Materials Science & Engineering A*, vol. 216, pp. 47-60 (1996).
12. Roplekar, J.K., & Dantzig, J.A., A Study of Solidification with a Rotating Magnetic Field," Int'l. Journal of Cast Metals Research, vol. 14, pp.79-95 (2001).
13. Geffroy, P.M, Lakehal, M., Goñi, J., Beargnon, E., Heintz, J.M. & Silvain, J.F., Thermal and Mechanical Behaviour of Al-Si Alloy Cast Using Magnetic Molding and Lost Foam Processes,", *Metallurgical and Materials Trans A,* vol. 37A, pp. 441-447 (2006).
14. Bustos, O., Ordoñez, S., & Colás, R., "Thermal and Microstructural Analysis of an A356 Aluminum Alloy Solidified Under the Effect of Magnetic Stirring," *International Journal of Metalcasting*, vol. 3, issue 3, pp. 37-41 (Summer 2009).
15. Chen, C.P. & Tsao, C.Y.A.,"Semi-Solid Deformation of Non-Dendritic Structures I. Phenomenological Behavior," *Acta Materialia*, vol. 45, issue 5, pp. 1955-1968 (1997).